nature COMMUNICATIONS

OPEN

ARTICLE

Received 19 Jan 2011 | Accepted 8 Jun 2011 | Published 5 Jul 2011

DOI: 10.1038/ncomms1378

Optical switching of nuclear spin–spin couplings in semiconductors

Atsushi Goto[1,2], Shinobu Ohki[1], Kenjiro Hashi[1] & Tadashi Shimizu[1]

Two-qubit operation is an essential part of quantum computation. However, solid-state nuclear magnetic resonance quantum computing has not been able to fully implement this functionality, because it requires a switchable inter-qubit coupling that controls the time evolutions of entanglements. Nuclear dipolar coupling is beneficial in that it is present whenever nuclear–spin qubits are close to each other, while it complicates two-qubit operation because the qubits must remain decoupled to prevent unwanted couplings. Here we introduce optically controllable internuclear coupling in semiconductors. The coupling strength can be adjusted externally through light power and even allows on/off switching. This feature provides a simple way of switching inter-qubit couplings in semiconductor-based quantum computers. In addition, its long reach compared with nuclear dipolar couplings allows a variety of options for arranging qubits, as they need not be next to each other to secure couplings.

[1] National Institute for Materials Science, 3-13 Sakura, Tsukuba, Ibaraki 305-0003, Japan. [2] PRESTO, Japan Science and Technology Agency, 4-1-8 Honcho, Kawaguchi, Saitama 332-0012, Japan. Correspondence and requests for materials should be addressed to A.G. (email: goto.atsushi@nims.go.jp).

Nuclear magnetic resonance (NMR) quantum computing has attracted broad interest because it is one of the most advanced testbeds for quantum computation. Although the interest began with solution NMR[1–3], it is now believed that scalable NMR quantum computers in the future will be built on semiconductors based on highly developed semiconductor technology[4–6]. The main challenges include the initialization and the creation of spin entanglement, which are essential features of quantum computation[7]. Semiconductor-based NMR quantum computers are advantageous as they can be achieved optically; that is, the initialization (nuclear–spin polarization) is provided by optical pumping[8,9], and the entanglement is created via internuclear (nuclear spin–spin) couplings between polarized nuclei[10,11]. In optically pumped semiconductors, the latter manifests itself as dipolar order[12,13] and double-quantum coherence[14].

Switchability is another essential functionality required for internuclear couplings, which should be 'on' during operations and 'off' otherwise. In this respect, nuclear dipolar coupling (*D*-coupling, hereafter) is not the best choice for the above-mentioned reasons. In addition, the time required for operations increases rapidly with increasing qubit number because of decoupling operations[15]. Other possible candidates include indirect couplings mediated by donor electrons[4] and magnons[15]. Their implementations are fairly challenging, however, given the complicated switching mechanisms. By contrast, the scheme presented in this paper is rather simple; the coupling strength can be controlled externally through light power, and on/off switching can be easily implemented.

In this study, we have preformed cross-polarization (CP) experiments with GaAs under light illumination, and demonstrated that a nuclear spin–spin coupling grows in strength, and extends its reach to farther nuclei as light power is increased. These futures bring about a unique transition of the CP process from oscillatory behaviour in the 'dark' towards exponential relaxation with increasing light power. The experiments provide us with information on the essential features of the optically induced nuclear spin–spin couplings; in particular, we find that the coupling strength is roughly proportional to light power, which is essential for the switching of the couplings.

Results

CP process in GaAs in the dark. The present mechanism is manifested in a CP process from ^{75}As (*I*-spin) to ^{71}Ga (*S*-spin) in GaAs under infrared light irradiation. Before detailing this process, we first describe it in the dark (without light irradiation) as a reference. This is an ordinary CP process, for which we expect a contact time (τ_{cp}) dependence of *S*-magnetization (M_S^{eq}) of the form

$$M_S^{eq}(\tau_{cp}) = M_0^{eq}[1-\exp(-\tau_{cp}/T_{IS})], \quad (1)$$

where T_{IS} is the cross-relaxation time. A relaxation process in the rotation frame ($T_{1\rho}$) need not be considered here, as it is sufficiently long because of high crystal symmetry[16,17]. The reality, however, is more complicated than equation (1). Figure 1 shows $M_S^{eq}(\tau_{cp})$ obtained in the dark, which exhibits a clear transient oscillation.

Transient oscillations have been reported in some molecular crystals, and attributed to discrete *S*–*I* coupling spectra of isolated *S*–*I* pairs[18–20]. The magnetization is transferred back and forth inside the pair with a frequency corresponding to half the flip-flop term of the *D*-coupling. The present sample, however, is not a molecular crystal, so isolated pairs are expected to be rare. Here an essential factor is the existence of two Ga isotopes, that is, ^{69}Ga and ^{71}Ga with natural abundances of $^{69}N_A = 0.604$ and $^{71}N_A = 0.396$, respectively. A local ^{75}As -^{71}Ga pair appears when only one of the four nearest-neighbour sites of ^{75}As is occupied by ^{71}Ga and the others are occupied by ^{69}Ga. The probability of finding such pairs is $_4C_1 \cdot {}^{71}N_A \cdot ({}^{69}N_A)^3 = 0.35$; that is, about 35% of ^{75}As have a single ^{71}Ga in the vicinity and contribute to the oscillation. The pairs are coupled through indirect scalar coupling J_{IS}, where *D*-couplings are absent because the Ga sites are situated at magic angle positions in the (100) crystal orientation[16,17,21]. The process is described by a damping oscillation[18],

$$M_S^{eq}(\tau_{cp}) = M_0^{eq}\left[1-\frac{1}{2}\exp(-R\tau_{cp})-\frac{1}{2}\exp(-3R\tau_{cp}/2)\cos(2\pi\Omega\tau_{cp})\right], \quad (2)$$

where Ω is the oscillation frequency ($\Omega = J_{IS}/2$) and R is the damping factor. We fit the data using equation (2) with Ω and R as free parameters. The best result is obtained with $\Omega = 0.74$ kHz, which yields $J_{IS} = 2\Omega = 1.48$ kHz. This value is comparable with that in the InP case ($J_{IS} = 2.3$ kHz)[17]. The fitting curve is shown by a solid line in Figure 1. The fit is not very good at the beginning of the oscillation; this may be due to the presence of ^{75}As sites with more than one ^{71}Ga nucleus in the four nearest-neighbour sites.

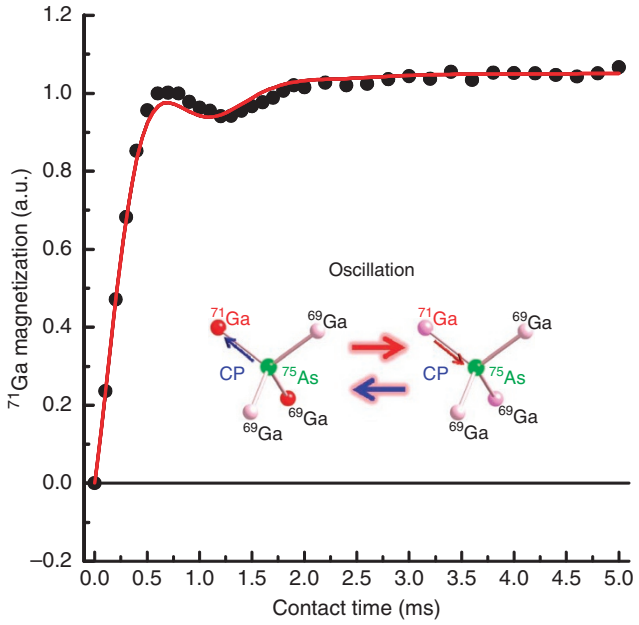

Figure 1 | CP experiment in GaAs in the dark. Contact time (τ_{cp}) dependence of ^{71}Ga magnetization (M_S^{eq}) in a cross polarization experiment in the dark at 10 K, normalized at $\tau_{cp} = 0.7$ ms. The pulse sequence is shown in Figure 5, where the light is turned off, that is, $P_{IR} = 0$ mW. The magnetization is transferred back and forth between ^{75}As and ^{71}Ga at a nearest neighbour site. This process gives rise to a transient oscillation. The solid red line represents the best-fit curve using equation (2).

CP process under light irradiation. Figure 2a shows the τ_{cp} dependence of *S*-polarization, $M_S(\tau_{cp})$ under various levels of light power, P_{IR}, which exhibits new local maxima (peaks) that are not observed in the dark. The maxima form a number of series (α, β, γ…), and the maximal position in each series shifts towards smaller values of τ_{cp} as the light power is increased. For example, the series 'β' shown by the red arrows starts with a broad maximum around $\tau_{cp} = 3.1$ ms at $P_{IR} = 100$ mW, which shifts towards smaller values of τ_{cp} as P_{IR} is increased and eventually merges into a peak at $\tau_{cp} = 0.8$ ms at 166 mW. These maxima represent new polarization transfer processes that appear under light irradiation. Figure 3 shows a three-dimensional representation of Figure 2a obtained by interpolating the data in between. The continuous shift of the maximum in each series can be readily confirmed.

This phenomenon can be explained by discrete increments in the number of *S*-nuclei (^{71}Ga) involved: in the dark ($P_{IR} = 0$ mW), the number of nuclei participating in the process is small and oscillatory behaviour is observed, as shown in Figure 1. Light illumina-

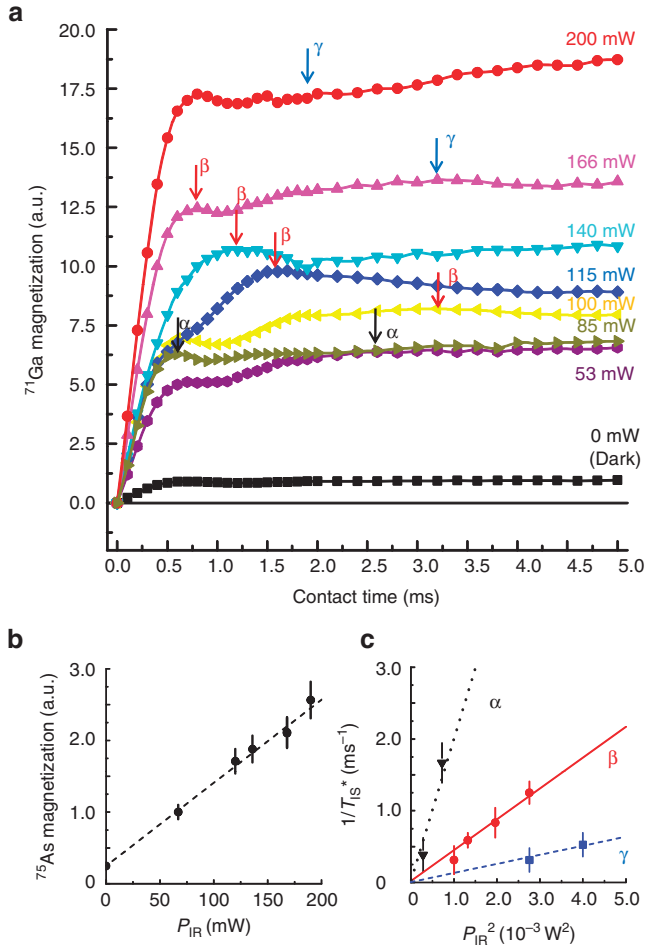

Figure 2 | CP experiments in GaAs under light irradiation. (**a**) Contact time (τ_{cp}) dependence of ^{71}Ga magnetization (M_s) in CP experiments at 10 K measured under light irradiation with power P_{IR} ranging from 0 to 200 mW. The pulse sequence is shown in Figure 5. The data at P_{IR} = 0 mW are the same as those in Figure 1. Black, red and blue arrows represent the three series of maxima. (**b**) The light power (P_{IR}) dependence of ^{75}As magnetization (M_I), which represents the enhancement of the nuclear spin polarization due to the optical pumping effect. The magnetization exhibits a linear dependence with P_{IR}. The error bars represent the data scatterings in a few experiments performed under the same conditions. (**c**) The values of $1/T_{IS}^*$ for the three series (α, β and γ) marked by the arrows in (**a**) plotted against P_{IR}^2. The error bars represent the breadth around each peak. The lines are visual guides.

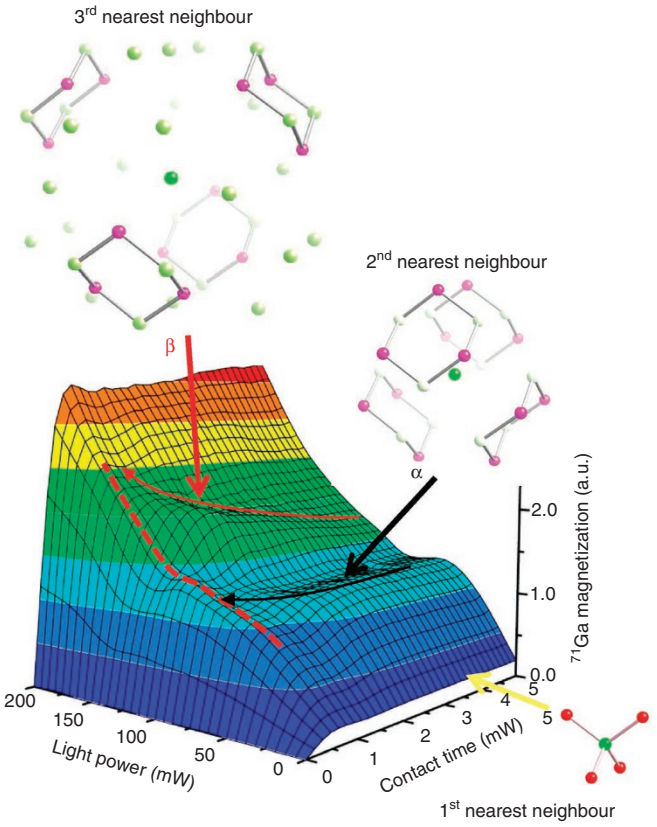

Figure 3 | Light power dependence of the CP process in GaAs. Three-dimensional representation of Figure 2a obtained by interpolating the data in between. The data shown by the yellow arrow represents those in the dark (P_{IR} = 0 mW), which corresponds to the polarization transfer to the nearest-neighbour ^{71}Ga through the conventional J_{IS}. The black (α) and red (β) arrows indicate the series of maxima corresponding, presumably, to the polarization transfers to the second and third nearest neighbour sites, respectively. The dotted red line represents the ^{71}Ga magnetization at τ_{cp} = 0.7 ms, which exhibits a plateau-like feature (that is, less steeper slope) around 80 mW.

tion causes a series of *S*-nuclei batches (α, β, γ…) to participate in sequence. Their contributions are successively added to the signal intensity one after another, whereas the speed of transfer from *I*- to *S*-nuclei in each series increases with the light power (that is, the maximal position shifts towards smaller values of τ_{cp}). As the number of nuclei involved is further increased, the cross relaxation is expected to approach the exponential relaxation behaviour given by equation (1)[20]. That is, we see here the transition from oscillatory behaviour in the 'dark' towards exponential relaxation with increasing light power. This is a unique case in that such a transition can hardly be observed in ordinary NMR measurements.

Another factor responsible for the phenomenon is the optical pumping effect[8,9]. It contributes to the *S*-magnetization (^{71}Ga) through the enhancement of the *I*-magnetization (^{75}As) caused by the polarization transfer from the optically oriented electrons for the duration of light irradiation τ_L = 60 s. Figure 2b shows the light-power dependence of the *I*-magnetization (^{75}As), which increases linearly with light power. This enhancement is partly responsible for the increase of the *S*-magnetization with increasing light power, as seen in Figures 2a and 3.

The τ_{cp} dependence of M_s is expressed as,

$$M_S(\tau_{cp}) = M_I^{dark}(\tau_L) m_{I\to S}^{eq}(\tau_{cp}) + M_I^{op}(P_{IR},\tau_L) \times \left[m_{I\to S}^{eq}(\tau_{cp}) + \sum_{i=\alpha} m_{I\to S}^{op,i}(P_{IR},\tau_{cp}) \right], \quad (3)$$

where $M_I^{dark}(\tau_L)$ in the first term on the right-hand side represents the *I*-magnetization in the dark portion of the sample recovered during τ_L = 60 s and $m_{I\to S}^{eq}$ represents the polarization transfer process to *S*-spins in the first nearest neighbour sites through J_{IS}. This process is essentially the same as that in Figure 1. On the other hand, $M_I^{op}(P_{IR},\tau_L)$ in the second term is the *I*-magnetization in the illuminated area generated by the optical pumping effect during τ_L = 60 s, whose P_{IR} dependence is shown in Figure 2b. This magnetization is transferred to *S*-spins through the two processes shown in the brackets: the same process as that in the dark, $m_{I\to S}^{eq}$, and additional ones induced by light irradiation, $\Sigma_i\, m_{I\to S}^{op,i}(P_{IR},\tau_{cp})$ (i = α, β, γ…). The latter are caused by the optically induced heteronuclear indirect coupling, J_{IS}^{opt}. We will discuss characteristics of this coupling in the next section.

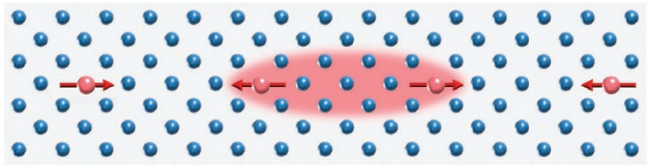

Figure 4 | Optical switching of a nuclear spin–spin coupling. A conceptual (ideal) model of optical switching of a nuclear spin–spin coupling between nuclear-spin qubits (red arrows) spaced a few lattice points apart from each other. Blue balls represent 'inert' (for example, spin-zero) nuclei. The nuclear dipolar couplings between the qubits are out of reach. Once the light is illuminated, a coupling emerges between the qubits. The strength of the coupling can be controlled externally through light power.

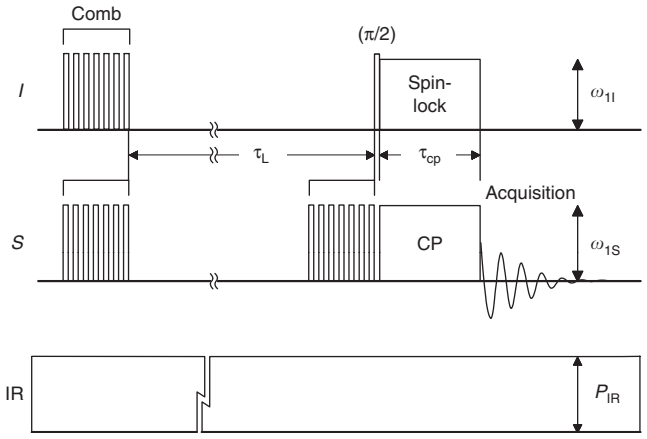

Figure 5 | Pulse sequence. Pulse sequence for optical pumping CP experiments. $I = {}^{75}$As, $S = {}^{71}$Ga and IR = infrared light (1.50 eV, σ^-). 'Comb': comb pulse consisting of a number of $\pi/2$ pulses. τ_L: duration of light irradiation (= 60 s). τ_{cp}: contact time for CP. $\omega_{1I}/2\pi$, $\omega_{1S}/2\pi$: rf-pulse strengths in terms of Rabi frequency (= 35 kHz). P_{IR}: infrared light power. The horizontal axis is not to scale.

Discussion

The new coupling J_{IS}^{opt} is presumably mediated by photo-excited electrons. It is known that electrons in metals can mediate indirect nuclear spin–spin couplings, a process referred to as the RKKY interaction[22]. In the present case, however, J_{IS}^{opt} is observed in semiconductors where no intrinsic Fermi surfaces exist. Moreover, the lifetimes and spin relaxation times of the photo-excited electrons usually fall in the range between pico- and nanoseconds, which is more than six orders of magnitude smaller than that of the CP process, that is, milliseconds. It is intriguing that two phenomena with such different time scales are coupled with each other.

The strength of J_{IS}^{opt} in each batch (α, β, γ…) can be evaluated by the cross-relaxation time T_{IS}^{opt} in $m_{I\to S}^{op,i}(P_{IR},\tau_{cp})$ (i = α, β, γ…). According to Demco *et al.*[17,20,23], the cross-relaxation time is expressed as

$$1/T_{IS}^{opt} \approx \frac{\sqrt{\pi}}{4} M_2^{IS} \tau_c, \qquad (4)$$

where τ_c is the correlation time of the CP and,

$$M_2^{IS} = \frac{1}{3} I(I+1) \sum (2\pi J_{IS}^{opt})^2 \qquad (5)$$

is the second moment of the I–S heteronuclear spectrum due to J_{IS}^{opt}. Equation (5) indicates that M_2^{IS} is proportional to $(J_{IS}^{opt})^2$. Provided that J_{IS}^{opt} is proportional to P_{IR} and that τ_c is independent of J_{IS}^{opt}, equations (4) and (5) lead to the conclusion that $1/T_{IS}^{opt}$ is proportional to P_{IR}^2. The actual value of T_{IS}^{opt} in each batch is determined from the analysis of the functional form of $m_{I\to S}^{op,i}(P_{IR},\tau_{cp})$ (i = α, β, γ…). Here we evaluate it from the maximal position; T_{IS}^{*} is defined as the contact time at which the maximum is formed. Figure 2c shows $1/T_{IS}^{*}$ for the three series of maxima (α, β and γ) plotted against P_{IR}^2. The graph suggests that $1/T_{IS}^{*}$ is roughly proportional to P_{IR}^2, implying that J_{IS}^{opt} is proportional to P_{IR}.

This result provides a clue to the nature of the series of S-nuclei batches (α, β, γ…). Equation (5) indicates that the condition $M_2^{IS} \propto (J_{IS}^{opt})^2$ is fulfilled only when all I–S pairs participating in the summation of the right-hand side share the same J_{IS}^{opt}, such that J_{IS}^{opt} can be taken out of the summation Σ. Therefore, each series may be assigned to the polarization transfers to a batch of S-spins at the same distance from the I-spin at the origin. Figure 3 illustrates this situation. For example, the α-maxima may be assigned to the second nearest-neighbour S-spins, the β-maxima to the third, and so forth. It is reasonable that equivalent S-spins in the same order situated at the same distance from the I-spin share the same scalar coupling with it. Moreover, the contributions from nuclei in the same order to the correlation time are partially cancelled out[17,20,23]. Therefore, the assumption that τ_c is independent of J_{IS}^{opt} may be a reasonable approximation.

The result also provides us with information about the reach of J_{IS}^{opt}. The dotted red line in Figure 3 shows the P_{IR} dependence of $M_s(\tau_{cp})$ at a constant τ_{cp}. One finds a plateau-like feature around 80 mW, which indicates that the S-spins at the third nearest-neighbour sites participate in the process only when $P_{IR} > 80$ mW; that is, J_{IS}^{opt} can reach farther than D- and J_{IS}-couplings, as the latter two may not substantially reach the third-nearest neighbours.

Features such as the external switchability and the long reach may add variety to the qubit arrangement in semiconductor-based NMR quantum computers. Figure 4 shows an example. In an array of nuclear–spin qubits, a few lattice points apart from each other, the D-couplings are out of reach, so that the qubits are decoupled. Then, the present mechanism provides the external control of internuclear couplings. As the light power is increased, the reach of couplings is extended. This would further enhance the flexibility of qubit arrangements.

This mechanism is compatible with most schemes proposed for semiconductor-based NMR quantum computing. The implantation of nuclear spin arrays in semiconductors has been studied using various techniques such as scanning probe microscopes, ion beams, and isotope engineerings[24–26]. These techniques will provide promising technologies to implement the schemes shown in Figure 4.

In conclusion, we have discovered an optically switchable indirect nuclear spin–spin coupling, which is manifested in CP experiments with GaAs under light illumination. As the strength of this coupling is externally controllable through light power, we expect it to have an essential role in the quantum gate operations of solid-state NMR quantum computers in the future.

Methods

Optical pumping double resonance NMR system and the sample. The CP experiments were performed at 10 K using an optical-pumping double-resonance NMR system developed for this study. The system consists of an NMR spectrometer, a laser system and a cryostat loaded in a 6.34-T superconducting magnet. A custom-built double-resonance probe is installed inside the cryostat. The sample used in this study is an undoped semi-insulating GaAs single-crystal wafer with a thickness of 600 μm and a crystal orientation of (100) (Mitsubishi Chemical). It is mounted on a sample stage made of sapphire located at the probe head and set with the surface normal to the magnetic field. The sample stage is cooled through thermal contact with the cold head of the cryostat. Infrared light emitted from a Ti:Sapphire laser is delivered to the cryostat through a polarization-maintaining fibre[27]. It is converted to circularly polarized light by a quarter-wave plate at the probe head, and applied to the sample in parallel to the magnetic field. The spot size at the sample surface is about ϕ5 mm.

Pulse sequence. The pulse sequence used is shown in Figure 5. The magnetization of I-spins, saturated by the first comb pulse, is regenerated during the time interval

τ_L and transferred to *S*-spins through the CP immediately thereafter. The infrared light is irradiated at a constant strength P_{IR} throughout the sequence. The photon energy of 1.50 eV (near the band gap) and the helicity σ^- were selected so that the optical pumping NMR signal enhancements for both ^{71}Ga and ^{75}As were nearly maximal. The experiment in the dark (Fig. 1) was obtained with the same pulse sequence as that in Figure 5, with the exception that $P_{IR} = 0$ mW.

References

1. Chuang, I. L., Gershenfeld, N. & Kubinec, M. Experimental implementation of fast quantum searching. *Phys. Rev. Lett.* **80,** 3408–3411 (1998).
2. Jones, J. A. & Mosca, M. Implementation of a quantum algorithm on a nuclear magnetic resonance quantum computer. *J. Chem. Phys.* **109,** 1648–1653 (1998).
3. Vandersypen, L. M. K., Steffen, M., Breyta, G., Yannoni, C. S., Sherwood, M. H. & Chuang, I. L. Experimental realization of Shor's quantum factoring algorithm using nuclear magnetic resonance. *Nature* **414,** 883–887 (2001).
4. Kane, B. E. A silicon-based nuclear spin quantum computer. *Nature* **393,** 133–137 (1998).
5. Shimizu, T., Goto, A., Hashi, K. & Ohki, S. An NMR quantum computer of the semiconductor CdTe. *Superlattice Microst.* **32,** 313–316 (2002).
6. Ladd, T. D., Goldman, J. R., Yamaguchi, F., Yamamoto, Y., Abe, E. & Itoh, K. M. All-silicon quantum computer. *Phys. Rev. Lett.* **89,** 017901 (2002).
7. DiVincenzo, D. P. Two-qubit gates are universal for quantum computation. *Phys. Rev. A* **51,** 1015–1022 (1995).
8. Tycko, R. & Reimer, J. A. Optical pumping in solid state nuclear magnetic resonance. *J. Phys. Chem.* **100,** 13240–13250 (1996).
9. Hayes, S. E., Mui, S. & Ramaswamy, K. Optically pumped nuclear magnetic resonance of semiconductors. *J. Chem. Phys.* **128,** 052203 (2008).
10. Doronin, S. I. Multiple quantum spin dynamics of entanglement. *Phys. Rev. A* **68,** 052306 (2003).
11. Rufeil-Fiori, E., Sanchez, C. M., Oliva, F. Y., Pastawski, H. M. & Levstein, P. R. Effective one-body dynamics in multiple-quantum NMR experiments. *Phys. Rev. A* **79,** 032324 (2009).
12. Michal, C. A. & Tycko, R. Nuclear spin polarization transfer with a single radio-frequency field in optically pumped indium phosphide. *Phys. Rev. Lett.* **81,** 3988–3991 (1998).
13. Tycko, R. Optical pumping of dipolar order in a coupled nuclear spin system. *Mol. Phys.* **95,** 1169–1176 (1998).
14. Patel, A. & Bowers, C. R. Two-dimensional nuclear magnetic resonance spectroscopy in optically pumped semiconductors. *Chem. Phys. Lett.* **397,** 96–100 (2004).
15. Goto, A., Shimizu, T., Hashi, K., Kitazawa, H. & Ohki, S. Decoupling-free NMR quantum computer on a quantum spin chain. *Phys. Rev. A* **67,** 022312 (2003).
16. Tomaselli, M., deGraw, D., Yarger, J. L., Augustine, M. P. & Pines, A. Scalar and anisotropic *J* interactions in undoped InP: a triple-resonance NMR study. *Phys. Rev. B* **58,** 8627–8633 (1998).
17. Goto, A., Hashi, K., Shimizu, T. & Ohki, S. Dynamics of electron-nuclear and heteronuclear polarization transfers in optically oriented semi-insulating InP: Fe. *Phys. Rev. B* **77,** 115203 (2008).
18. Muller, L., Kumar, A., Baumann, T. & Ernst, R. R. Transient oscillations in NMR cross-polarization experiments in solids. *Phys. Rev. Lett.* **32,** 1402–1406 (1974).
19. Hester, R. K., Ackerman, J. L., Cross, V. R. & Waugh, J. S. Resolved dipolar coupling spectra of dilute nuclear spins in solids. *Phys. Rev. Lett.* **34,** 993–995 (1975).
20. Mehring, M. *Principles of High Resolution NMR in Solids* (Springer, 1983).
21. Iijima, T., Hashi, K., Goto, A., Shimizu, T. & Ohki, S. Homonuclear and heteronuclear indirect spin-spin couplings in InP studied using ^{31}P cross polarization NMR spectra under magic-angle spinning. *Jpn. J. Appl. Phys. Part 2* **42,** L1411–L1413 (2003).
22. Ruderman, M. A. & Kittel, C. Indirect exchange coupling of nuclear magnetic moments by conduction electrons. *Phys. Rev.* **96,** 99–102 (1954).
23. Demco, D. E., Tegenfeldt, J. & Waugh, J. S. Dynamics of cross relaxation in nuclear magnetic double resonance. *Phys. Rev. B* **11,** 4133–4151 (1975).
24. Schenkel, T. Semiconductor physics: reliable performance. *Nature Mater.* **4,** 799–800 (2005).
25. Ruess, F. J. *et al.* Toward atomic-scale device fabrication in silicon using scanning probe microscope. *Nano Lett.* **4,** 1969–1973 (2004).
26. Itoh, K. M. An all-silicon linear chain NMR quantum computer. *Solid State Commun.* **133,** 747–752 (2005).
27. Goto, A., Ohki, S., Hashi, K. & Shimizu, T. Optical-pumping double-resonance NMR system for semiconductors. *Rev. Sci. Instrum.* **77,** 093904 (2006).

Acknowledgements

We acknowledge C. Takizawa for technical assistance. We also acknowledge High Magnetic Field Station (Tsukuba Magnet Laboratory), NIMS, and Niki Glass for their support. This work was partially supported by JST PRESTO program. K.H. was supported by a Grant-in-Aid for Scientific Research (No. 20540323) from the Japan Society for the Promotion of Science.

Author contributions

A.G. conceived and designed the experiments. All the authors jointly designed the system for the experiments, and A.G. and S.O. constructed it. A.G. carried out the main experiments. All the authors were involved in the analyses. A.G. wrote the paper, with the help of the co-authors.

Additional information

Competing financial interests: The authors declare no competing financial interests.

Reprints and permission information is available online at http://npg.nature.com/reprintsandpermissions/

How to cite this article: Goto, A. *et al.* Optical switching of nuclear spin–spin couplings in semiconductors. *Nat. Commun.* 2:378 doi: 10.1038/ncomms1378 (2011).